



Published in final edited form as:

*J Phys Chem C Nanomater Interfaces*. 2010 January 8; 114(16): 7432–7435. doi:10.1021/jp910627r.

## Optical Properties of Nested Pyramidal Nanoshells

Julia Y. Lin<sup>†</sup>, Warefta Hasan<sup>†</sup>, Jiun-Chan Yang<sup>†</sup>, and Teri W. Odom<sup>†,‡,\*</sup>

<sup>†</sup>Department of Chemistry, Northwestern University, 2145 Sheridan Road, Evanston, Illinois 60208-3113

<sup>‡</sup>Department of Materials Science and Engineering, Northwestern University, 2145 Sheridan Road, Evanston, Illinois 60208-3113

### Abstract

This paper describes the fabrication and characterization of nested Au pyramidal nanoshells. These particles exhibited two plasmon resonances at visible and near-infrared wavelengths that could be manipulated depending on the size of the gap between inner and outer pyramidal shells. We found that larger gaps (30 nm) exhibited much larger Raman scattering responses compared to smaller gaps (5 nm) in the nested pyramidal shells. The SERS-activity of these anisotropic particles can be optimized by adjusting the distances between the inner and outer Au shells.

---

Metal nanoparticles (NPs) exhibit characteristic localized surface plasmon (LSP) resonances that are tunable by varying intrinsic factors such as material, shape, size and extrinsic ones such as the local dielectric environment.<sup>1, 2</sup> When small particles (diameter,  $d < 50$  nm) are separated by distances less than the diameter of an individual NP, the LSPs of one particle can interact with those of the other through dipolar coupling.<sup>3</sup> For example, the plasmon resonance of isolated Au disks can split into lower and higher energy resonances when two disks are separated by a few nanometers ( $< 5$  nm).<sup>4</sup> Multi-layered Au-dielectric-Au disks (thicknesses = 10-10-10 nm) exhibit two plasmon resonances because of coupling between the upper and lower particles.<sup>5</sup> When the thickness of the dielectric spacer is decreased to less than 6 nm, the optical response is similar to that of a single Au disk (thickness = 20 nm).<sup>5, 6</sup> Thus, as the separation between two NPs decreases, the plasmon coupling increases, and the LSP resonances shift to lower energies (red-shift to longer wavelengths).<sup>4</sup> Changes in the optical properties from particle-particle coupling are important in biodiagnostics,<sup>7</sup> optoelectronic devices,<sup>8</sup> and nonlinear spectroscopies.<sup>9</sup>

The intense, localized electromagnetic fields that occur between closely spaced particles as a result of plasmon coupling can serve as hot spots for enhanced Raman scattering.<sup>10, 11</sup> Hence, NP assemblies and pairs of NPs<sup>10, 12, 13</sup> are ideal plasmonic structures for surface enhanced Raman scattering (SERS) and single molecule sensing.<sup>10, 14</sup> Despite reports of Raman enhancements by nanoparticle clusters,<sup>10–13</sup> the formation of well-defined NP aggregates has not been controlled. Specifically, the overall spatial environment—the size of the NP assemblies, the organization of the NPs in the assemblies, and the separation between the particles—is difficult to manipulate. Fabrication approaches, however, provide routes to control the size and spacing of gaps between nanostructures, which can lead to reproducible SERS-active particles and substrates.<sup>15, 16</sup>

---

\*To whom correspondence should be addressed. [todom@northwestern.edu](mailto:todom@northwestern.edu).

**Supporting Information Available.** Table of Au and Cr content in the nested pyramids after Cr etching. Large-area Raman and SEM images of solid 40-nm Au, nested (gaps = 5 nm and 10 nm), and Au-Cr-Au pyramidal shells. This material is available free of charge via the Internet at <http://pubs.acs.org>.

Here we describe the fabrication, optical characterization, and SERS response of nested pyramidal nanoshells. These NPs are composed of two pyramidal shells, where a smaller shell is stacked inside a larger shell, and whose flat faces are parallel and separated by a gap. We found that the nested pyramids exhibited plasmon resonances at visible and near-infrared wavelengths that could be manipulated by increasing the gap distance between the shells. Interestingly, the nested pyramids showed optical properties that were similar to those of a single Au pyramidal shell of the same total metal thickness, but the resonances were blue-shifted by 50–75 nm. Also, we discovered that the gap distance between the inner and outer shells controlled the Raman scattering response. Nested particles with larger gaps (30 nm) exhibited SERS intensities greater than solid pyramidal shells or nested pyramidal shells with smaller gaps (5 nm).

Nested pyramidal nanoshells were fabricated by Phase-shifting photolithography, Etching, E-beam, and Lift-off (PEEL)<sup>17</sup> followed by a post-etching step. Multi-layered pyramids composed of two Au layers surrounding a sacrificial material layer (Cr) were first created, and then the Cr was etched to create the nested pyramids. Figure 1 is a scheme of the fabrication procedure to create nested pyramidal nanoshells. In brief, a thin Ti film perforated with 250–300-nm diameter holes was used as both an etching and deposition mask. The underlying Si (100) wafer was first anisotropically etched to form pyramidal-shaped pits, and then alternating layers of Au and Cr were evaporated through the nanoholes. Multi-layered Au-Cr-Au (thicknesses = 20-45-20 nm) pyramids were generated containing 51% Au; 49% Cr (atomic %) as determined by electron dispersive spectroscopy (EDS) (Figs. 2a, b). After the Ti film was removed, the nanopyramid/Si template was immersed in a Cr etchant (Transene, diluted 1:3 with water) to dissolve the Cr in the multi-layered Au-Cr-Au pyramids and to result in nested pyramidal nanoshells (Figs. 2c–e). Nested nanoshells with gap distances of 5 nm (100% Au; 0% Cr) were formed after 80 s in the Cr etchant, and nested particles with gaps of 30 nm (75% Au; 25% Cr) were formed after 30 s. We used focused ion beam (FIB) milling to view cross-sections of the nested pyramidal shells. Figures 2a and c reveal that even after etching, the gap distance between the Au shells remained constant.

To carry out single particle, dark field (DF) scattering measurements (Fig. 3a), the nested pyramids were removed from the Si template by dry etching in gaseous XeF<sub>2</sub> (XACTIX, Inc.) followed by sonication in water. Samples were prepared by dispersing the nested pyramidal nanoshells on indium tin oxide (ITO)-coated glass substrates patterned with Au alignment markers so that the particle orientation determined by SEM images could be correlated to the DF scattering spectra. A broadband white light source (100 W, halogen lamp) was used to illuminate the particles through a DF condenser, and the light scattered from the nested pyramids was collected by a variable numerical aperture objective (100×, NA = 0.5) and dispersed by a spectrometer equipped with a liquid N<sub>2</sub>-cooled CCD. All spectra were taken in air ( $n = 1.00$ ) to ensure a uniform dielectric environment within the gap and around the particles (excluding the substrate).

Similar to what we observed in previous work,<sup>18, 19</sup> we found that the nested pyramidal shells adopted two orientations when dispersed on a flat substrate: (1) tips pointing up and away from the surface, and (2) tips pointing down or touching the surface. Particles in each orientation exhibited distinct spectral features that can be used to predict the directionality of the pyramidal tips on a substrate.<sup>19</sup> Figures 3b-c compare the orientation-dependent optical properties of a Au-Cr-Au multi-layered pyramid (thicknesses = 20-45-20 nm), a nested pyramidal shell (gap = 30 nm; total Au thickness = 40 nm), and a Au single shell pyramid (thickness = 40 nm). The spectra of the Au-Cr-Au pyramid in the tip-up orientation showed broad features at 550 nm and 800 nm (Fig. 3b). Optical spectra of tip-down Au-Cr-Au particles (Fig. 3c), however, were not as sharp as those observed for the tip-up Au-Cr-Au pyramids. Substrate effects could

explain the additional broadening of the spectral features in the tip-down Au-Cr-Au pyramids.<sup>20, 21</sup>

The resonances of tip-up nested pyramidal shells were red-shifted compared to the Plasmon resonances of the Au-Cr-Au pyramids in the same orientation. The optical response of the tip-up and tip-down nested pyramidal shells were similar in shape, and the resonances occurred around the same wavelengths. One difference is that an additional peak appeared as a shoulder in the spectrum of the tip-down nested pyramidal shells at 725 nm (Fig. 3c). Because the particles were dispersed on a substrate, there was a slight anisotropy in the refractive index environment around the particle. Hence, the outer shell of the nested nanoshells was strongly affected by the non-uniform surroundings (ITO-coated glass substrate ( $n = 1.80$ ) and air ( $n = 1.00$ )). The feature at 725 nm could be a result of this local dielectric asymmetry.

To evaluate the effects of coupling between the inner and outer shells of the nested pyramids, we systematically etched the Cr in the Au-Cr-Au multi-layered pyramids (Fig. 4). As the Cr was removed, the interactions between the shells increased. We determined the relative compositions of Au and Cr by EDS and correlated the % Cr with etching times (Supporting Information, Table S1). For both tip-up and tip-down nested pyramid orientations, the resonances red-shifted as the Cr layer was etched; however, tip-up particles exhibited greater peak shifts (Fig. 4a) compared to tip-down ones (Fig. 4b) because of reduced contact with the substrate.<sup>20</sup> Notably, after the formation of the initial gap, subsequent changes in Cr composition did not shift the resonances much until after the Cr was completely etched and the structure collapsed (Fig. 2f and Fig. 4a). The spectral features of the collapsed, nested pyramids and solid pyramidal shells were similar; hence, the 5-nm gap is too small to affect the resonances significantly.

The localized EM fields confined between inter-particle junctions are favorable for enhancing Raman scattering.<sup>10, 11, 13</sup> We investigated how the gap distance between the inner and outer pyramidal shells affected the SERS response of a Raman reporter molecule methylene blue (0.5 mM) adsorbed uniformly on the nested particle surfaces. Raman images were collected with a confocal Raman microscope (Alpha, WiTec Instruments) using 633-nm excitation (He-Ne laser, Coherent Inc.). Because the SERS signal depends on particle orientation with respect to the polarization of the laser,<sup>22</sup> the pyramids were left in the Si template so that only the effects of the gaps could be compared and so that any tip-effects were avoided (unpublished results).

Figure 5 compares Raman images from four different pyramidal structures: (1) solid 40-nm Au pyramidal shells, (2) collapsed, nested pyramids (gap = 5 nm), (3) nested pyramids (gap = 30 nm), and (4) multi-layered Au-Cr-Au pyramids. Large-area, confocal Raman images were taken to ensure that the signal was representative for each of the pyramidal structures (Supporting Information, Fig. S1). We found that pyramids without gaps (Fig. 5a) did not exhibit a SERS response. In contrast, the collapsed, nested pyramids showed some Raman scattering (Fig. 5b), although the signal was much weaker (the intensity of the  $1621\text{ cm}^{-1}$  C-C ring stretching mode was 60 times lower) than the nested pyramids with 30-nm gaps (Fig. 5c). Previous work on Au nanorods suggested that the decrease in SERS activity observed in particles separated by smaller gaps (a few nanometers) was from the detuning of the dipolar and multipolar modes.<sup>16</sup> Hence, a 5-nm separation may be too small to affect the Raman scattering of molecules within the gap. Additionally, we interrogated the Au-Cr-Au pyramids to examine any possible damping effects of Cr<sup>23, 24</sup> on the SERS signal. Although the Au-Cr-Au multi-layered particles revealed weak Raman scattering (Fig. 5d), the signal was still greater (by 5 times) than that from a single Au or a collapsed, nested pyramidal particle. Consequently, the SERS signal could result from the Au roughness at the Au-Cr interfaces or the small-gap volume created between inner and outer shells because of the slightly recessed

Cr layer (Fig. 2a). Overall, these results are in agreement with SERS experiments on methylene blue and gold nanodisk wires using 633-nm light.<sup>16</sup> We also carried out measurements at 785 nm to investigate the wavelength-dependence of the Raman signal; however, no enhancement was observed.

In summary, we have reported a controllable method to produce nested pyramidal nanoshells. The optical properties of these particles can be altered by varying the distance between the inner and outer pyramidal shell layers. We demonstrated that nested pyramidal nanoshells with large gaps (tens of nanometers) are promising for SERS applications because they support a large Raman-active volume. Because the location and intensity of hotspots can be tuned by changing the separation between inner and outer shells, we anticipate that these results will be useful in designing improved SERS-based chemical and biological sensors.

## Supplementary Material

Refer to Web version on PubMed Central for supplementary material.

## Acknowledgments

This work was supported in part by the NSF NSEC program at Northwestern University (EEC-0647560), the David and Lucile Packard Foundation, and the NIH Director's Pioneer Award (DP1OD003899). This work used the NUANCE Center facilities, which are supported by NSF-MRSEC, NSF-NSEC and the Keck Foundation. We thank the Mirkin group and M. Pedano (Northwestern) for assistance with confocal Raman microscopy.

## References

1. Link S, El-Sayed MA. *J. Phys. Chem. B* 1999;103:8410–8426.
2. Kelly KL, Coronado E, Zhao LL, Schatz GC. *J. Phys. Chem. B* 2003;107:668–677.
3. Jensen T, Kelly L, Lazarides A, Schatz GC. *J. Cluster Sci* 1999;10:295–317.
4. Atay T, Song J-H, Nurmikko AV. *Nano Lett* 2004;4:1627–1631.
5. Dmitriev A, Pakizeh T, Käll M, Sutherland DS. *Small* 2007;3:294–299. [PubMed: 17199248]
6. Henzie J, Lee MH, Odom TW. *Nat Nano* 2007;2:549–554.
7. Elghanian R, Storhoff JJ, Mucic RC, Letsinger RL, Mirkin CA. *Science* 1997;277:1078–1081. [PubMed: 9262471]
8. Quinten M, Leitner A, Krenn JR, Aussenegg FR. *Opt. Lett* 1998;23:1331. [PubMed: 18091775]
9. Shalaev VM, Poliakov EY, Markel VA. *Phys. Rev. B* 1996;53:2437.
10. Nie SM, Emery SR. *Science* 1997;275:1102. [PubMed: 9027306]
11. Jiang, Bosnick K, Maillard M, Brus L. *J. Phys. Chem. B* 2003;107:9964.
12. Camden JP, Dieringer JA, Wang Y, Masiello DJ, Marks LD, Schatz GC, Van Duyne RP. *J. Am. Chem. Soc* 2008;130:12616. [PubMed: 18761451]
13. Michaels AM, Jiang, Brus L. *J. Phys. Chem. B* 2000;104:11965.
14. Kneipp K, Wang Y, Kneipp H, Perelman LT, Itzkan I, Dasari RR, Feld MS. *Phys. Rev. Lett* 1997;78:1667.
15. Fromm DP, Sundaramurthy A, Kinkhabwala A, Schuck PJ, Kino GS, Moerner WE. *J. Chem. Phys* 2006;124
16. Qin L, Zou S, Xue C, Atkinson A, Schatz GC, Mirkin CA. *Proc. Natl. Acad. Sci. U. S. A* 2006;103:13300. [PubMed: 16938832]
17. Henzie J, Kwak E-S, Odom TW. *Nano Lett* 2005;5:1199. [PubMed: 16178210]
18. Henzie J, Shuford KL, Kwak E-S, Schatz GC, Odom TW. *J. Phys. Chem. B* 2006;110:14028. [PubMed: 16854094]
19. Hasan W, Lee J, Henzie J, Odom TW. *J. Phys. Chem. C* 2007;111:17176.
20. Dmitriev A, Häggglund C, Chen S, Fredriksson H, Pakizeh T, Käll M, Sutherland DS. *Nano Lett* 2008;8:3893. [PubMed: 18844428]

21. Knight MW, Wu Y, Lassiter JB, Nordlander P, Halas NJ. *Nano Lett* 2009;9:2188. [PubMed: 19361166]
22. McLellan JM, Li Z-Y, Siekkinen AR, Xia Y. *Nano Lett* 2007;7:1013. [PubMed: 17375965]
23. Jiao X, Goeckeritz J, Blair S, Oldham M. *Plasmonics* 2009;4:37.
24. Aouani H, Wenger J, Gérard D, Rigneault H, Devaux E, Ebbesen TW, Mahdavi F, Xu T, Blair S. *ACS Nano* 2009;3:2043–2048.

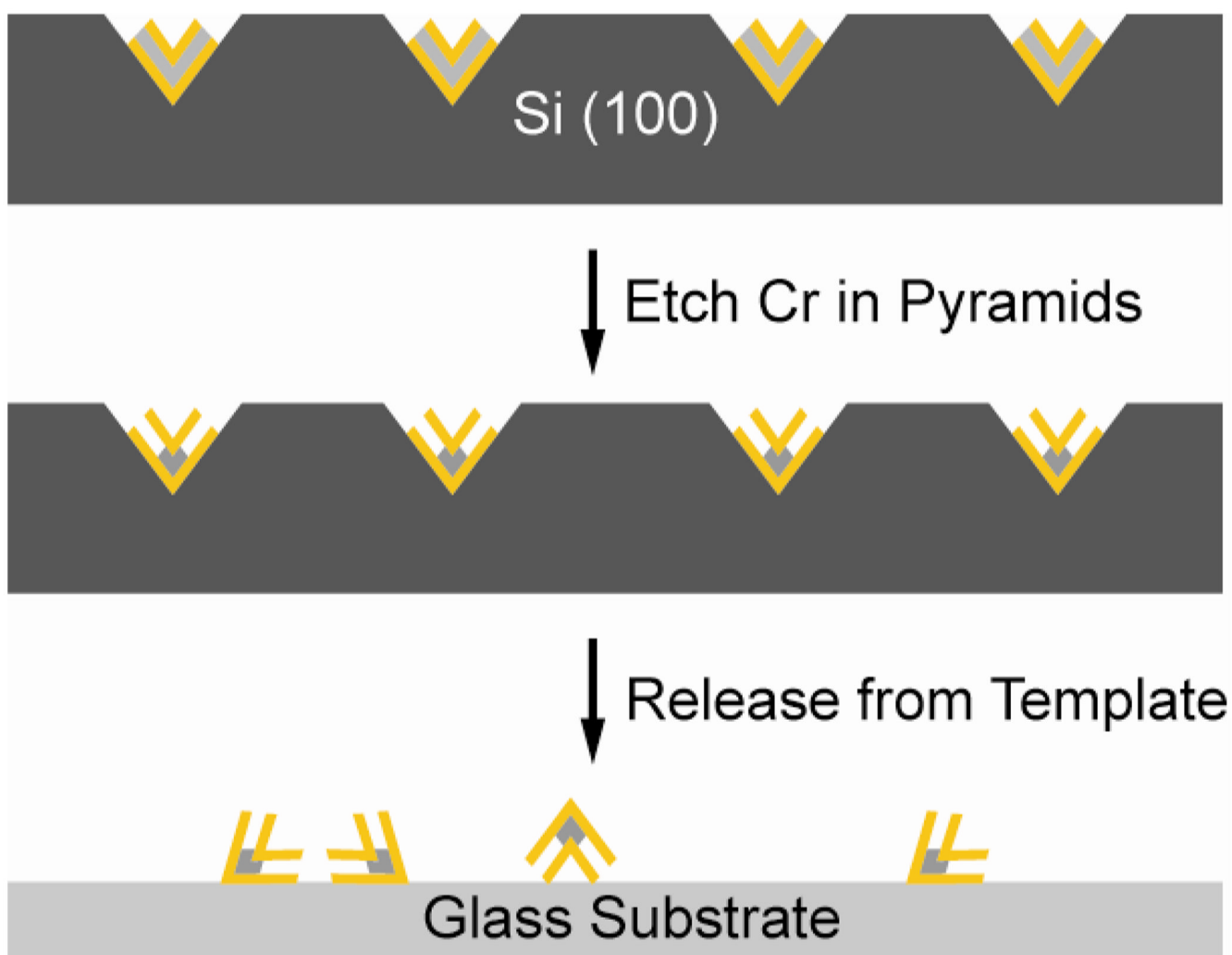


**Figure 1.**  
Scheme depicting the fabrication strategy for creating nested pyramidal nanoshells.

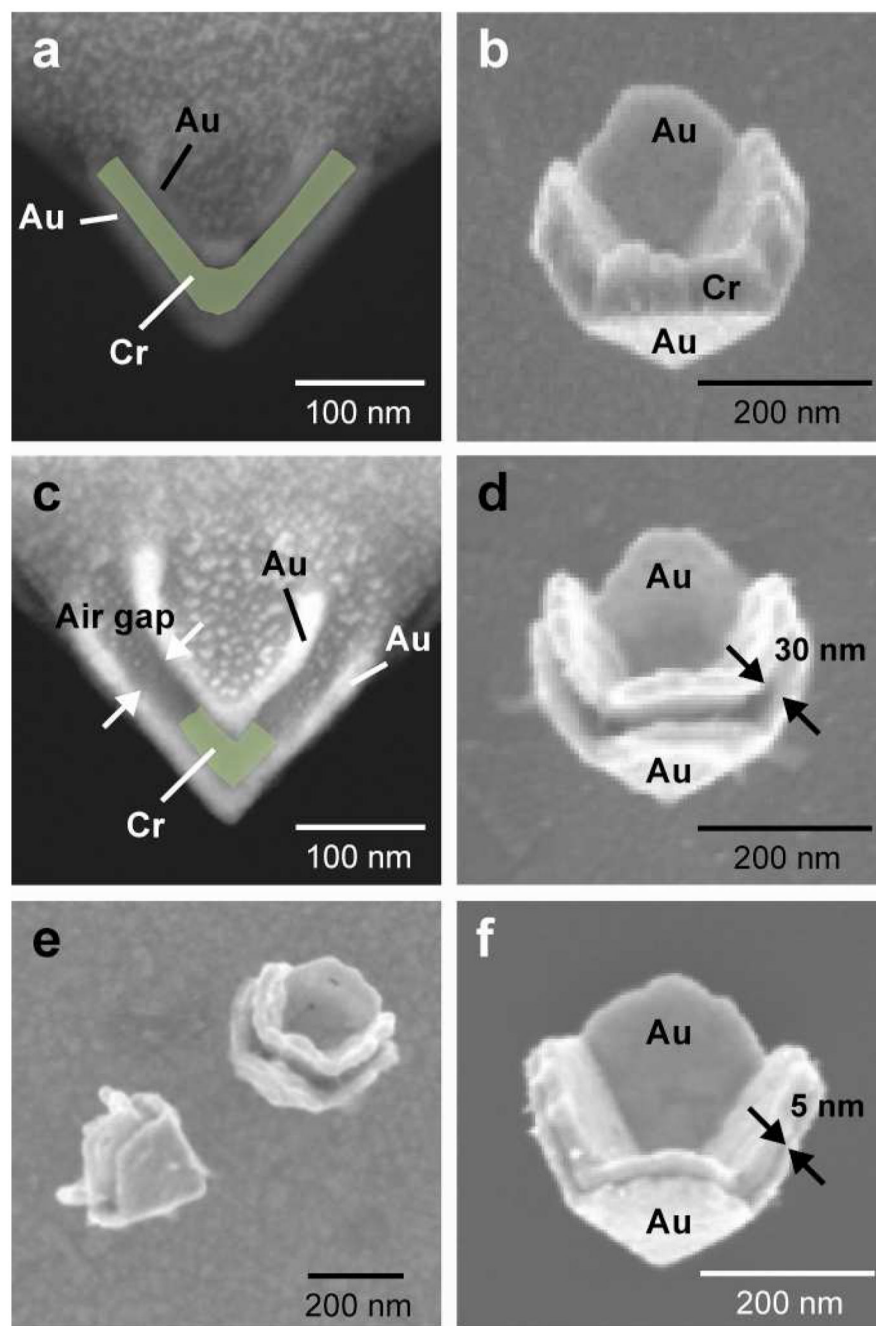


**Figure 2.**

Scanning electron microscopy (SEM) images of (a–b) FIB-milled cross-section in Si template and free-standing Au-Cr-Au (20-45-20 nm) multi-layered pyramids. (c–d) Cross-section in template and free-standing nested pyramidal nanoshell (gap = 30 nm). (e) Tip-down orientation of nested pyramidal nanoshells. (f) A collapsed, nested pyramid particle (gap = 5 nm).

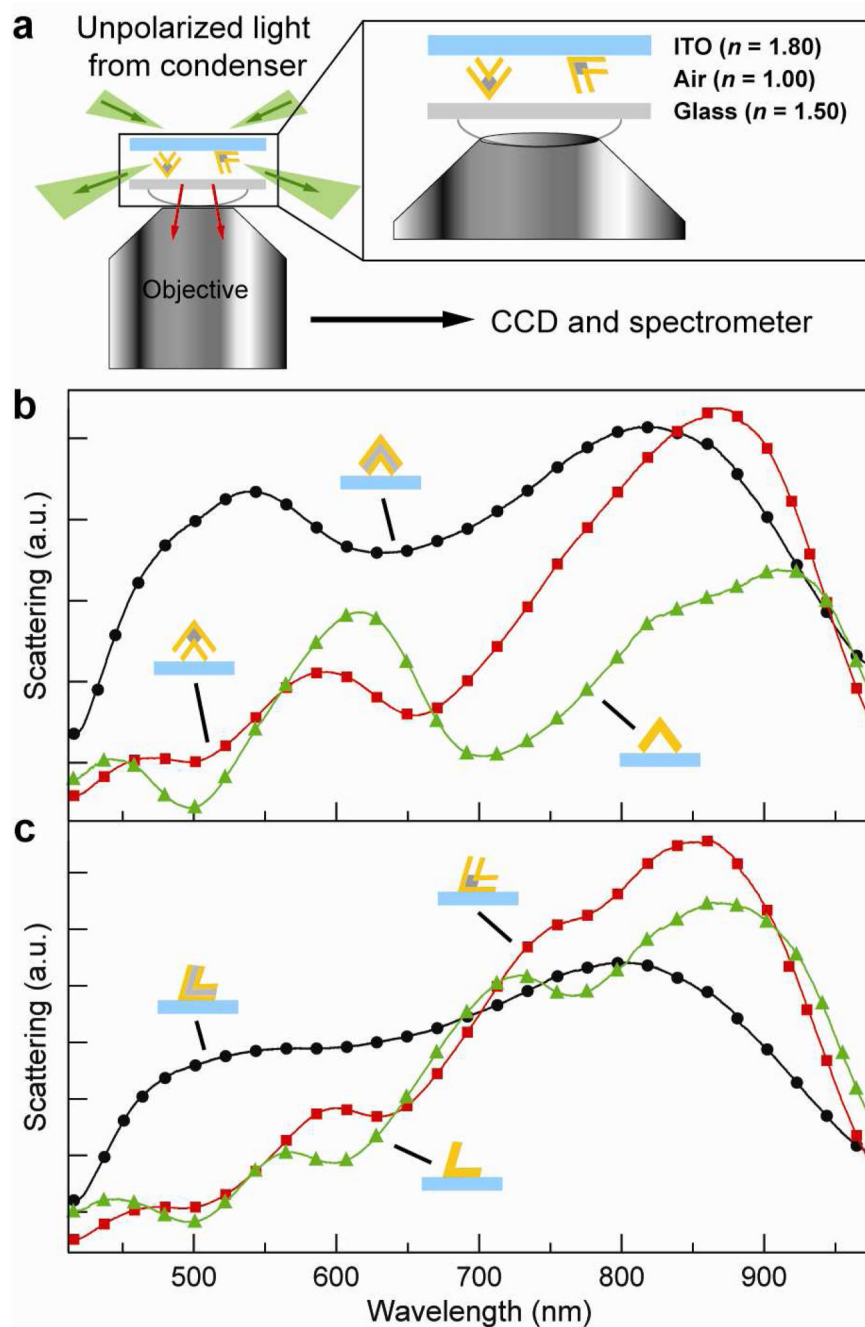


**Figure 3.** (a) Single particle scattering spectroscopy set-up. Optical spectra of (b) tip-up and (c) tip-down nested pyramidal nanoshells and a single Au pyramid shell (thickness = 40 nm). Particle diameters were ca. 280 nm.



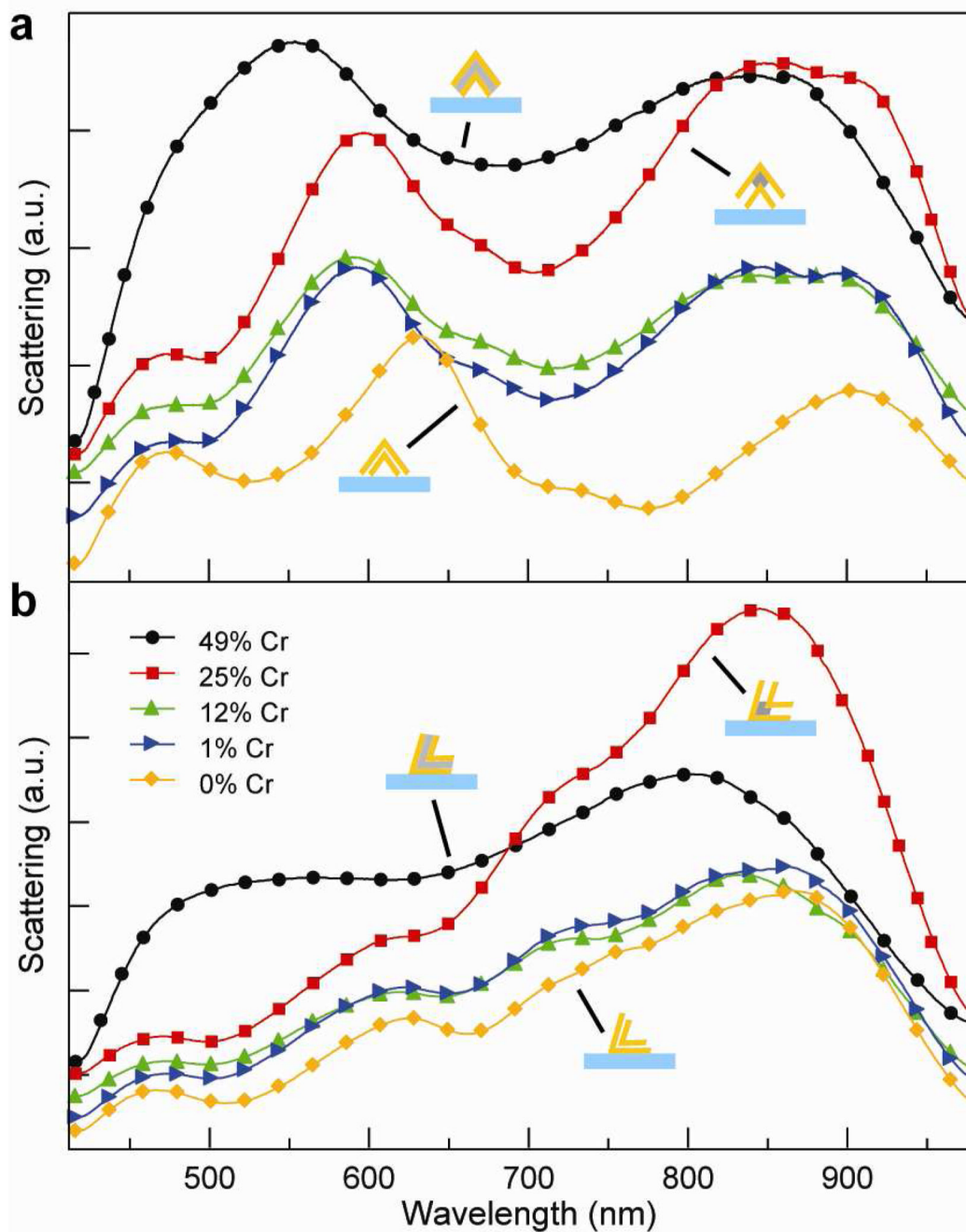


**Figure 4.** Scattering spectra of single nested pyramidal nanoshells as the Cr content was decreased by chemical etching. Starting particles were Au-Cr-Au (20-45-20 nm). (a) Tip-up and (b) tip-down orientations. Spectra were offset for clarity.

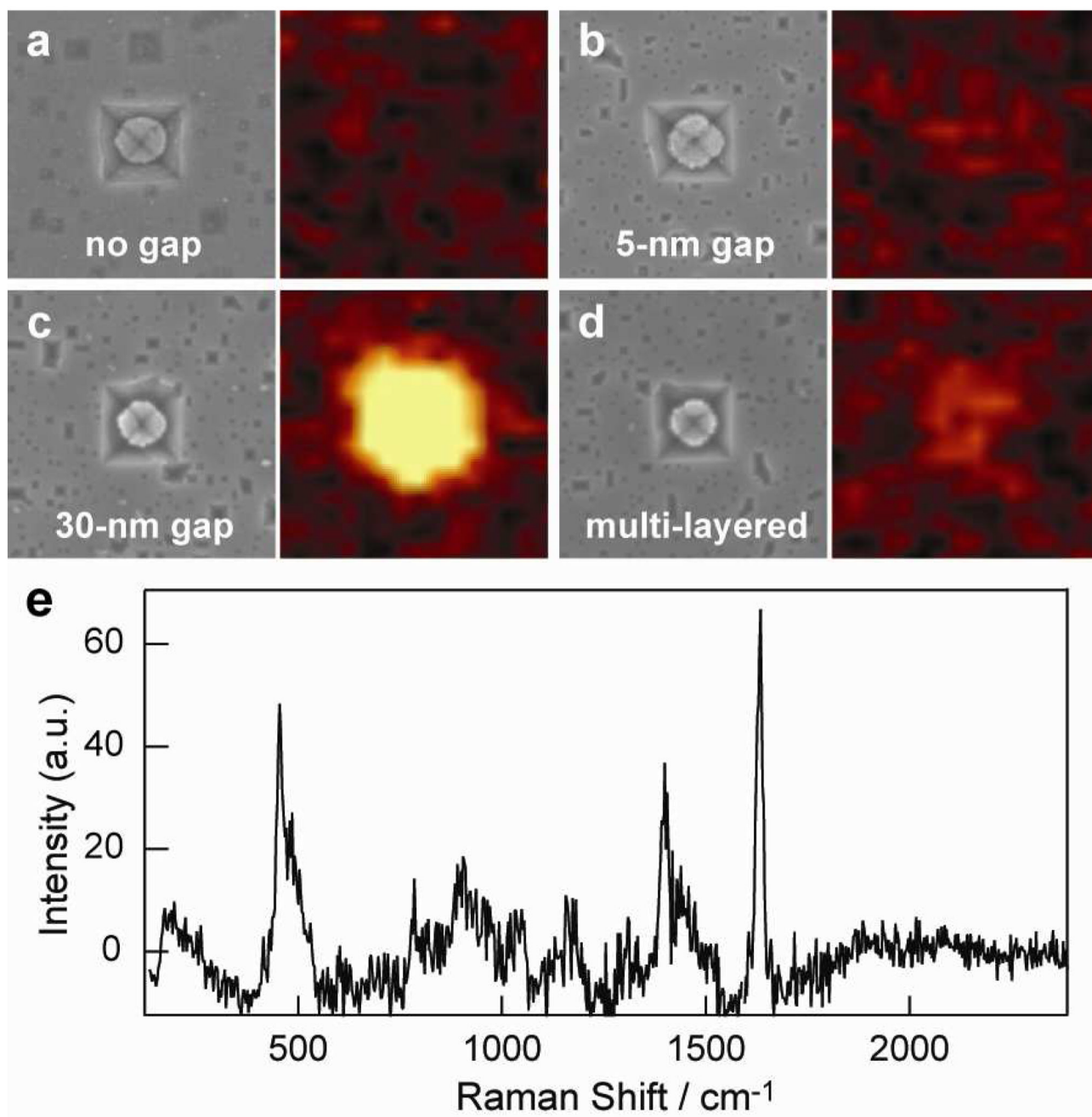


**Figure 5.**

SEM images (left) and corresponding Raman images (right) of (a) a single Au pyramid shell (thickness = 40 nm), (b) a collapsed, nested pyramidal particle (gap = 5 nm), (c) a nested pyramidal particle (gap = 30 nm), and (d) a Au-Cr-Au (20-45-20 nm) multi-layered pyramid. The confocal Raman and SEM image areas are  $1.5 \mu\text{m} \times 1.5 \mu\text{m}$ . (e) Representative SERS spectrum of methylene blue acquired from (c).